Dynamic Fluorescence Probing of the Microenvironment of Sodium Dodecyl Sulfate Micelle Solutions: Surfactant Concentration Dependence and Solvent Isotope Effect

Hideaki Shirota,*,†,‡ Yushi Tamoto,§ and Hiroshi Segawa‡,§

Department of General Systems Sciences, Graduate School of Arts & Sciences, University of Tokyo, 3-8-1 Komaba, Meguro-ku, Tokyo 153-8902, Japan, and Department of Applied Chemistry, Graduate School of Engineering, University of Tokyo, 3-8-1 Komaba, Meguro-ku, Tokyo 153-8902, Japan

Received: June 30, 2003; In Final Form: December 13, 2003

We have studied the surfactant concentration dependence and solvent isotope effect on the slow solvation dynamics and orientational dynamics of solvatochromic coumarin dyes in the aqueous sodium dodecyl sulfate (SDS) micelle solutions using picosecond fluorescence spectroscopy. The solvation time constants for SDS micelle H_2O solutions are about 130 ps and 2.5 ns. Both the faster and slower solvation time constants do not depend on the SDS concentration in the range 16.2−810 mM, though the observed solvation component becomes larger with increasing of SDS concentration. The solvation dynamics in SDS micelle D_2O solutions is about 1.2 times slower than that in SDS micelle H_2O solutions. The retardation of the solvation dynamics in micelle solutions could be due to the slower process of the hydrogen bond dynamics in the hydration layer around the micelle, as well as simple hydrogen-bonding liquids. The surfactant concentration dependence and solvent isotope effect on the orientational dynamics of the fluorescence probe is correlated with those on the solvation dynamics in SDS micelle solutions.

1. Introduction

Hydration water shows the very different properties, such as viscosity, polarity, pH, freezing point, and mobility, compared with those of bulk water due to the specific interactions and microenvironments and the presence of salts and ions.[1−3] Because the water molecules in hydration play a key role on controlling the structure, dynamics, functionality, and activity in biological systems, the dynamical process of water in complex systems has been extensively studied.[3−8] Especially, the dynamics of water in surfactant self-organized molecular assembly systems has been paid great attention, because they are simple models of biological membranes.[7]

Micelles, the subject of this work, are one of the typical surfactant self-organized molecular assembly systems.[9,10] It is well-known that some amphiphilic surfactants in water form micelles due to the hydrophobic interaction. The hydration layer, so-called the Stern layer, exists in the interface between the hydrophobic micelle core and bulk water. This layer consists of the ionic headgroups, counterions, and hydrated water molecules. The layer should play an important role for the structural stability and dynamical property of micelles in water.

One of the effective and useful methods to characterize the dynamical feature of condensed phases is the time-dependent fluorescence Stokes shift measurement of a solvatochromic fluorescence probe.[11−13] When a suitable fluorescence molecule, which shows a linear correlation between the fluorescence maximum and a solvent polarity, is used as a probe, the time-dependent spectral correlation function $S(t)$ is given by

$$S(t) = \frac{\nu_{fl}(t) - \nu_{fl}(\infty)}{\nu_{fl}(0) - \nu_{fl}(\infty)} \quad (1)$$

where $\nu_{fl}(t)$, $\nu_{fl}(0)$, and $\nu_{fl}(\infty)$ are the frequencies of fluorescence maximum at time t, 0, and ∞, respectively. Namely, $t = 0$ is the time at which the electronic excitation occurs and $t = \infty$ corresponds to the time when the equilibrium of the solvent reorganization process of the medium molecules around the excited-state probe molecule has been reached. Because of the recent availability of the short pulse light source, it has made it possible to observe the solvation dynamics of pure solvents at ambient temperature.[12−17] The interest in the solvation dynamics is now extended to complex systems[7,8,18−22] including surfactant assembly systems, such as micelles,[23−29] reverse micelles,[30−52] vesicles,[53−56] Langmuir layers,[57−60] and micelle−polymer complexes.[61−63]

The extremely slow solvation dynamics in normal micelle solutions was experimentally found by Bhattacharrya and coworkers.[23,24] They measured the solvation dynamics in anionic sodium dodecyl sulfate (SDS), cationic cetyl trimethylammonium bromide (CTAB), and neutral Triton X-100 (TX-100) micelle solutions. The solvation dynamics in micelle solutions is variable by the hydration layer. The component of the slow solvation dynamics due to the hydration layer in the TX-100 micelle solution is the largest among these three micelle solutions. This is because the hydration layer in the TX-100 micelle solution is much thicker than that in SDS and CTAB micelle solutions, because TX-100 has the large hydrophilic part of the $(-CH_2CH_2O-)_n$ ($n = 9.4$). Within the good agreement with their result, Frauchiger et al. observed the large component of the slow solvation dynamics in an amphiphilic starlike macromolecule, which is composed mostly of poly(etlylene

* Corresponding author. E-mail: shirota@rutchem.rutgers.edu.
† Present address: Department of Chemistry & Chemical Biology, Rutgers University, 610 Taylor Road, Piscataway, NJ 08854.
‡ Department of General Systems Sciences.
§ Department of Applied Chemistry.

10.1021/jp035861j CCC: $27.50
Published on Web 03/19/2004

oxide), solution.[64] Very recently, the femtosecond solvation dynamics in CTAB and TX-100 micelle solutions was reported by Mandal et al.[25] Zewail and co-workers also measured the ultrafast solvation dynamics in CTAB and TX-100 micelle solutions as the mimics of the hydration layers of biological systems.[65,66]

The retardation of the orientational dynamics of water molecules in micelle solutions was also observed in the molecular dynamics simulation results. Recently, Bagchi and co-workers studied the dynamical feature of water molecules in cesium pentadecafluorooctanoate micelle solution.[27−29] Interestingly, they suggested that the retardation of the water dynamics near the micelle surface could be due to the contributions of the extended hydrogen bonds in water molecules with the headgroups of surfactants and of the quasi-bound water molecules. Berkowitz and co-workers reported the dynamical feature in SDS micelle solution.[67] They found that although the translational diffusion coefficient of water molecules in the first solvation shell around the micelle is reduced by less than a half of that in bulk water, the slow reorientation is slowed by 1 or 2 orders of magnitude.

Although there are some reports regarding the solvation dynamics in aqueous micelle solutions as mentioned above, the effects of the physical and chemical conditions, such as surfactant concentration, temperature, alkyl chain length, etc., on the solvation dynamics in micelle solutions are still unknown. In this work, we have investigated the surfactant concentration dependence and medium deuterium isotope effect on the solvation dynamics in SDS micelle solutions to understand the details of the solvation process in SDS micelle solutions. It is well-known that nearly spherical micelles in the spherical assembly concentration region do not show the surfactant concentration dependence on the diameter and surfactant aggregation number of a micelle, though the density of micelles and the mean distance between micelles vary. When the mean distance between micelles is competitive to the diameter of micelle, the hydration water molecules of a micelle should interact with the hydration water molecules of the other micelles. On the other hand, the hydration water of micelles in a dilute solution can access to the bulk water molecules for the long mean distance between micelles. It is interesting to see how the dynamics of the hydration water of micelles is affected by the surfactant concentration. We have also studied the solvent deuterium isotope effect on the solvation dynamics in SDS micelle solutions, because the deuterium isotopic substitution study is a useful method to investigate the role of hydrogen bonds on the static and dynamic features of hydrogen-bonding molecular systems.[1,13,68,69]

2. Experimental Section

SDS (Nacalai Tesque, >99%), laser-grade coumarin 102 and coumarin 153 (C102 and C153, both Exciton) were used without further purification (Figure 1). H_2O with the conductivity of 18.2 MΩ cm was obtained from a MilliQ system. D_2O (Isotech, 99.9%D) and Na_2SO_4 (Wako Pure Chemicals) were used as received. The concentration of coumarin dyes in micelle solutions were kept at about 0.02 mM, except for C102 in neat H_2O and D_2O (about 0.01 mM). The sample solutions were mixed by sonication and filtered through a 0.45 μm pore PTFE filter. The steady-state absorption and fluorescence spectra of the coumarin dyes in SDS micelle solutions were measured with a JASCO V-570 UV/vis/near-IR spectrometer and a JASCO FP-777 spectrofluorometer, respectively. The diameters of the micelles were estimated by dynamic light scattering measurements (Otsuka Electronics, DLS-70). The diameter of the SDS micelle is about 5.6 nm (5.0 ± 1 to 6.3 ± 2 nm) and does not vary with the SDS concentration and the deuterium substitution of medium within experimental error.

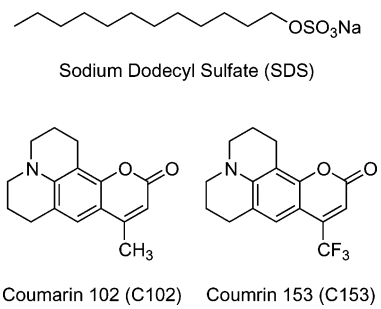

Figure 1. Chemical structures of sodium dodecyl sulfate (SDS), coumarin 102 (C102), and coumarin 153 (C153).

Details of the picosecond laser apparatus system were reported elsewhere.[70] Briefly, the fundamental light of a femtosecond titanium:sapphire laser (Spectra Physics, Tsunami) at about 800 nm with an average power of about 350 mW was used as the light source. A combined type doubler and pulse picker (Spectra Physics, Model 3980) was used to reduce the repetition frequency (from 82 to 4 MHz) and to produce the second harmonic light at about 400 nm. The sample was excited by the second harmonic light after passing though a Glan-Laser polarizer to set at the vertical polarization angle. The fluorescence of the sample was passed though a 2 mm slit attached with a 1 cm cell, a Glan-Laser polarizer set at the magic, horizontal, or vertical angle to the polarization of the pump beam, and a polychromator (Jobin Yvon CP-200) and was detected by a streak camera (Hamamatsu Photonics, C4334). The full widths at half-maxima of the instrument's responses were 20−30 ps for the 2 ns full-scale detection, 35−45 ps for the 5 ns full-scale detection, and 200−300 ps for the 20 ns full-scale detection. All the measurements were made at ambient temperature (295 ± 2 K).

3. Results

3.1. Steady-State Absorption and Fluorescence Spectra of Coumarin Dyes in SDS Micelle Solutions. Figure 2 shows the SDS concentration dependence on the steady-state absorption and fluorescence spectra of (a) C102 in SDS/H_2O solutions. The critical micelle concentration of SDS in H_2O is 8.1 mM, and even the highest SDS concentration of the samples used in the present study (810 mM) shows spherical micelles in solution.[71] It is clear from Figure 2a that both the absorption and fluorescence maxima of C102 shift dramatically at the SDS concentration of 8.1 mM, which is the critical micelle concentration for SDS in water. The absorption maximum shifts to the longer wavelength, and the fluorescence maximum shifts to the shorter wavelength when the SDS concentration is beyond the critical micelle concentration. Both the absorption and fluorescence maxima of C102 in SDS micelle solutions with SDS concentrations of ≥16.2 mM show only a tiny shift. Although C153 is not very soluble in pure water, C153 is highly soluble in SDS micelle solutions. The SDS concentration dependence of the steady-state absorption and fluorescence spectra of C153 in SDS micelle solutions ([SDS] = 8.1, 16.2, 81.0, 405, and 810 mM) shows features similar to those of C102. The steady-state absorption ν_{abs} and fluorescence ν_{fl} maxima and Stoke shift $\Delta\nu$ ($=\nu_{abs} - \nu_{fl}$) of C102 and C153 in SDS micelle solutions are listed in Table 1. We have also estimated the excitation light wavelength dependence on the steady-state

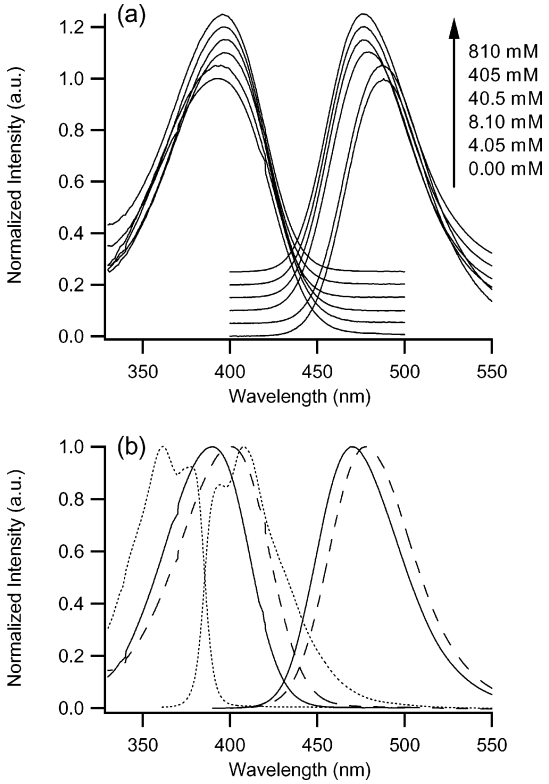

Figure 2. Steady-state absorption and fluorescence spectra of C102 in (a) aqueous SDS solutions with [SDS] = 0, 4.05, 8.10, 40.5, 405, and 810 mM (from bottom to top) and (b) pure solvents: cyclohexane (dots), methanol (solid lines), and glycerol (broken lines).

TABLE 1: Steady-State Absorption ν_{abs} and Fluorescence ν_{fl} Maxima and Stokes Shifts $\Delta\nu$ of C102 and C153 in SDS/H_2O and SDS/D_2O

dye	[SDS] (mM)	medium	$10^{-3}\nu_{abs}$/cm^{-1} (λ_{abs}/nm)	$10^{-3}\nu_{fl}$/cm^{-1} (λ_{fl}/nm)	$10^{-3}\Delta\nu$/cm^{-1}
C102	0.00	H_2O	25.48 (392.5)	20.48 (488.2)	5.00
	1.62	H_2O	25.45 (392.9)	20.50 (487.7)	4.95
	4.05	H_2O	25.42 (393.4)	20.52 (487.4)	4.90
	8.10	H_2O	25.20 (396.8)	20.84 (479.8)	4.38
	16.2	H_2O	25.19 (397.1)	20.96 (477.1)	4.23
	40.5	H_2O	25.20 (396.9)	20.96 (477.0)	4.24
	81.0	H_2O	25.21 (396.7)	20.96 (477.0)	4.25
	405	H_2O	25.24 (396.2)	20.97 (476.8)	4.27
	810	H_2O	25.26 (395.9)	20.98 (476.6)	4.28
C153	16.2	H_2O	22.96 (435.6)	18.72 (534.3)	4.24
	40.5	H_2O	22.96 (435.5)	18.72 (534.3)	4.24
	81.0	H_2O	22.96 (435.5)	18.72 (534.2)	4.24
	405	H_2O	23.01 (434.6)	18.73 (533.9)	4.28
	810	H_2O	23.05 (433.8)	18.74 (533.6)	4.31
C102	0.00	D_2O	25.48 (392.4)	20.48 (488.2)	5.00
	16.2	D_2O	25.19 (397.1)	20.96 (477.1)	4.23
	405	D_2O	25.25 (396.1)	20.97 (476.8)	4.28
C153	16.2	D_2O	22.97 (435.4)	18.71 (534.4)	4.26
	405	D_2O	23.02 (434.4)	18.73 (534.0)	4.29

fluorescence spectra of C102 (370, 400, and 420 nm) and C153 (400, 435, and 470 nm) in aqueous SDS micelle solutions with [SDS] = 16.2 and 405 mM. They do not depend on the excitation light wavelength within experimental error. The steady-state absorption and fluorescence spectra of C102 in cyclohexane, methanol, and glycerol are also shown in Figure 2b as the references.

The saturated concentrations of C102 in aqueous Na_2SO_4 solutions with several Na_2SO_4 concentrations have been measured. Because Na_2SO_4 is a simple model compound of the headgroup of SDS, it can estimate the effect of the ionic

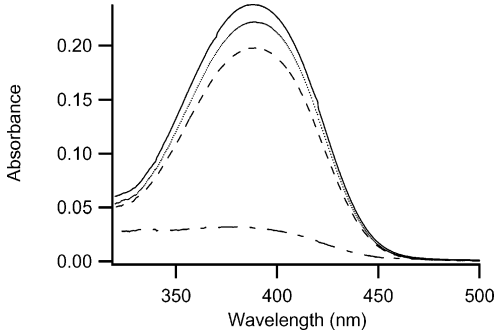

Figure 3. Concentration dependence on the steady-state absorption spectra of saturated C102 in aqueous Na_2SO_4 solutions. Solid line, dotted line, broken line, and dotted and broken line indicate [Na_2SO_4] = 0.0 (pure water), 0.01, 0.1, and 1.0 M, respectively.

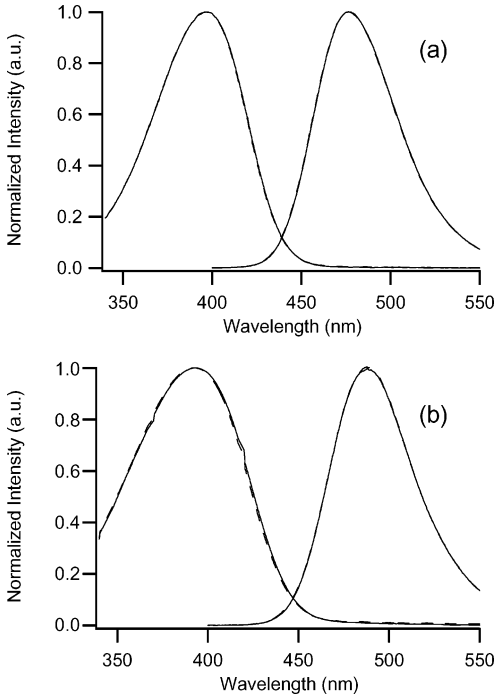

Figure 4. Steady-state absorption and fluorescence spectra of C102 in (a) SDS micelle solutions with the SDS concentration of 405 mM (solid lines for H_2O medium and broken lines for D_2O medium) and (b) pure H_2O (solid lines) and D_2O (broken lines).

environment. Figure 3 shows the steady-state absorption spectra of the saturated C102 in aqueous Na_2SO_4 solutions with [Na_2SO_4] = 0 (pure water), 0.01, 0.10, and 1.0 M. The solubility of C102 in aqueous Na_2SO_4 solution is decreasing with the higher Na_2SO_4 concentration, as shown in Figure 3. The ion concentration of the Stern layer in SDS micelle solutions is nearly similar to that of the aqueous Na_2SO_4 solution with the highest concentration.

Figure 4 shows the steady-state absorption and fluorescence spectra of C102 (a) in SDS/H_2O (solid lines) and SDS/D_2O (broken lines) with [SDS] = 405 mM and (b) in pure H_2O (solid lines) and D_2O (dotted lines). As shown in Figure 4 (a), the steady-state absorption and fluorescence spectra of C102 in SDS/D_2O are almost identical with those in SDS/H_2O within experimental error. Another concentration sample ([SDS] = 16.2 mM) also shows no deuterium isotope effects on the steady-state absorption and fluorescence spectra of C102 in SDS micelle solutions. The steady-state absorption and fluorescence spectra of C102 in pure D_2O are also almost identical with those in pure H_2O (Figure 4b). The steady-state absorption and fluorescence spectra C153 in SDS micelle solutions also show

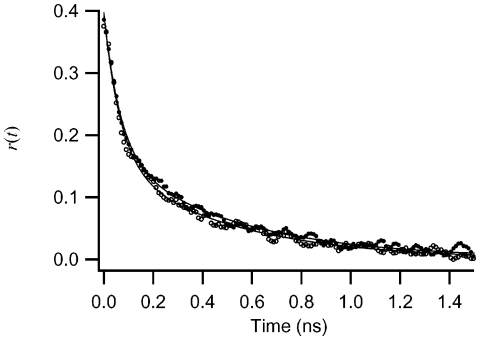

Figure 5. Fluorescence anisotropy decays $r(t)$ of C102 in SDS micelle solutions with the SDS concentrations of 16.2 mM (filled circles) and 405 mM (open circles). Biexponential fit curves are also shown.

TABLE 2: Reorientation Parameters for C102 and C153 in H_2O, D_2O, SDS/H_2O, and SDS/D_2O

dye	[SDS] (mM)	medium	a_{r1}[a]	τ_{r1} (ps)[a]	a_{r2}[a]	τ_{r2} (ps)[a]	$\langle\tau_r\rangle$ (ps)	$\langle\tau_r\rangle_D/\langle\tau_r\rangle_H$
C102	0.00	H_2O	0.38	59			59	
		D_2O	0.39	72			72	1.22
	16.2	H_2O	0.22	67	0.16	492	246	
		D_2O	0.19	75	0.19	548	312	1.27
	405	H_2O	0.22	66	0.17	496	253	
		D_2O	0.19	72	0.19	558	315	1.25
C153	16.2	H_2O	0.21	69	0.19	553	299	
		D_2O	0.20	74	0.19	651	355	1.19
	405	H_2O	0.23	70	0.17	550	274	
		D_2O	0.20	71	0.18	565	305	1.11

[a] Experimental error is ±10%, except for pure H_2O and D_2O (±5%).

no deuterium isotope effects. The steady-state absorption and fluorescence maxima and Stokes shifts of C102 and C153 in SDS/D_2O are listed in Table 1.

3.2. Fluorescence Depolarization Decays of Coumarins in SDS Micelle Solutions. The orientational dynamics of a fluorescence probe can be estimated by the fluorescence anisotropy decay measurements.[72]

$$r(t) = \frac{I_{||}(t) - I_{\perp}(t)}{I_{||}(t) + 2I_{\perp}(t)} \qquad (2)$$

where $I_{II}(t)$ and $I_{\perp}(t)$ are the tail-matched fluorescence transients polarized parallel and perpendicular to the polarization of the excitation light. To get the tail-matched fluorescence transients, the measured perpendicular fluorescence transients were multiplied by the calibration factor for the detector sensitivities to the polarized lights (1.13). Figure 5 shows the $r(t)$ of C102 in SDS micelle solutions with [SDS] = 16.2 and 405 mM. As shown in the figure, the fluorescence anisotropy decays of C102 in the SDS micelle solutions with [SDS] = 16.2 and 405 mM are almost overlapped. The biexponential fit curves ($a_{r1}\exp(-t/\tau_{r1}) + a_{r2}\exp(-t/\tau_{r2})$) are also shown in Figure 5. The reorientation time constants of C102 in SDS micelle solutions are about 70 and 500 ps (Table 2). The time constants of the fluorescence anisotropy decay for C153 in SDS micelle solutions are about 70 and 550 ps, and the orientational dynamics of C153 is also insensitive to the SDS concentration.

Figure 6 shows the $r(t)$ for C102 in SDS/H_2O and SDS/D_2O with [SDS] = 405 mM. The reorientation of C102 in SDS/D_2O is slower than that in SDS/H_2O. Another fluorescence probe molecule C153 and the different SDS concentration sample ([SDS] = 16.2 mM) also show similar deuterium isotope effects on the orientational dynamics of the fluorescence probes. The average reorientation time $\langle\tau_r\rangle$, which is defined as ($a_{r1}\tau_{r1} + a_{r2}\tau_{r2}$)/($a_{r1} + a_{r2}$), of the coumarins in SDS/D_2O is about 1.2 times larger than that in SDS/H_2O (Table 2). The $r(t)$ for C102 in pure H_2O and D_2O can be expressed by a single-exponential fit. The reorientation time constants for C102 in pure H_2O and D_2O are 59 and 72 ps, respectively.

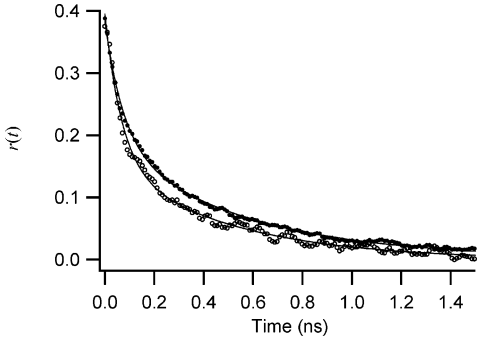

Figure 6. Comparison between the fluorescence anisotropy decays $r(t)$ of C102 in SDS H_2O and D_2O solutions with the SDS concentration of 405 mM (solid lines for H_2O medium and broken lines for D_2O medium). Biexponential fit curves are also shown.

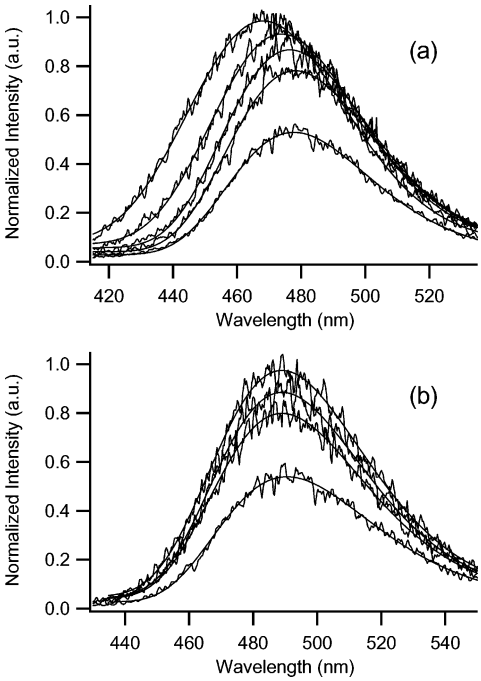

Figure 7. Time-resolved fluorescence spectra of C102 in (a) 405 mM SDS micelle solution at t = 0.03, 0.12, 0.30, 1.0, and 3.0 ns and (b) water at t = 0.03, 0.30, 1.0, and 3.0 ns.

3.3. Dynamic Fluorescence Stokes Shifts of Coumarins in SDS Micelle Solutions. Figure 7a shows the time-resolved fluorescence spectra of C102 in SDS micelle solution with [SDS] = 405 mM at times of 0.03, 0.12, 0.30, 1.0, and 3.0 ns. The fluorescence maximum shifts to the longer wavelength with the time evolution. The time-dependent Stokes shift of the fluorescence spectrum of C102 in pure H_2O is not observed as shown in Figure 7b, because the solvation dynamics in pure H_2O occurs much faster than the instrument's temporal response of the spectroscope used in this study.[15] The fluorescence maximum of the time-resolved fluorescence spectrum at each time is estimated from the fit by a log-normal line shape function.[73]

$$I_f(\nu) = I_{f0}\exp\left[-\ln(2)\left(\frac{\ln[1 + 2b(\nu - \nu_p)/\Delta]}{b}\right)\right] \qquad (3)$$

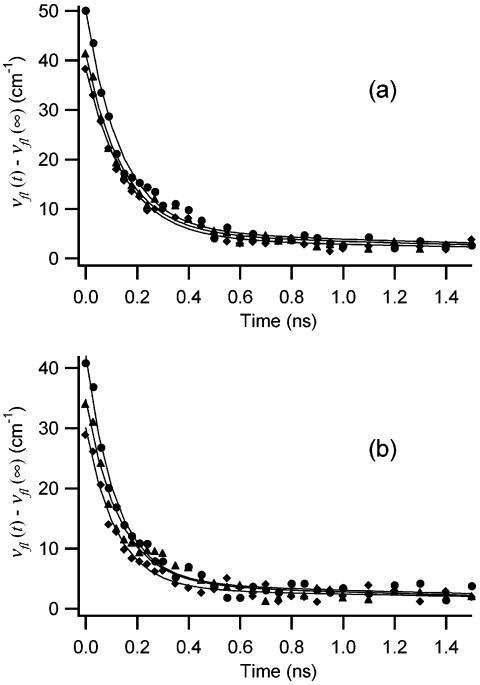

Figure 8. The time-dependent fluorescence maximum frequency shifts of (a) C102 and (b) C153 in SDS micelle solutions. Circles, triangles, and diamonds show [SDS] = 810, 81.0, and 16.2 mM, respectively. Biexponential fit curves are also shown.

TABLE 3: Dynamic Solvation Parameters for C102 and C153 in SDS/H_2O and SDS/D_2O

dye	[SDS] (mM)	medium	a_{s1}[a]	τ_{s1} (ns)[b]	a_{s2}[c]	τ_{s2} (ns)[d]	$\langle\tau_s\rangle$ (ns) ($\langle\tau_s\rangle_D/\langle\tau_s\rangle_H$)	obsd component
C102	16.2	H_2O	0.89	0.15	0.11	2.46	0.40	0.23
	40.5		0.87	0.15	0.13	2.46	0.45	0.24
	81.0		0.87	0.14	0.13	2.34	0.43	0.25
	405		0.89	0.15	0.11	2.68	0.43	0.28
	810		0.88	0.14	0.12	2.54	0.43	0.29
C153	16.2		0.89	0.12	0.11	2.57	0.39	0.18
	40.5		0.87	0.13	0.13	2.62	0.45	0.19
	81.0		0.87	0.13	0.13	2.43	0.43	0.22
	405		0.88	0.13	0.12	2.57	0.42	0.25
	810		0.89	0.12	0.11	2.52	0.38	0.26
C102	16.2	D_2O	0.89	0.18	0.11	3.16	0.51 (1.28)	0.24
	405		0.88	0.17	0.12	3.20	0.53 (1.23)	0.30
C153	16.2		0.88	0.15	0.12	2.88	0.48 (1.23)	0.18
	405		0.87	0.14	0.13	3.05	0.52 (1.24)	0.22

[a] Experimental error is ±5%. [b] Experimental error is ±10%. [c] Experimental error is ±10%. [d] Experimental error is ±15%.

where I_{f0}, ν_p, b, and Δ are the peak height, peak frequency, asymmetric parameter, and width parameter, respectively. When $2b(\nu - \nu_p)/\Delta$ is less than -1, $I_f(\nu)$ is taken as 0. The log-normal function fit curves are also shown in Figure 7.

Figure 8 shows the temporal shift of the time-resolved fluorescence maximum with the offset of the fluorescence maximum at the infinite time, $\nu_{fl}(t) - \nu_{fl}(\infty)$, for (a) C102 and (b) C153 in SDS micelle solutions with [SDS] = 16.2, 81.0, and 810 mM. Although all the data are in the 0−10 ns time range, we show the 1−1.5 ns time window for an easy view to understand the differences. The biexponentail fit ($a_{s1}\exp(-t/\tau_{s1}) + a_{s2}\exp(-t/\tau_{s2})$; $a_{s1} + a_{s2} = 1$) is made at the 1−10 ns time range, and data sets are also shown in Figure 8. The fit parameters are listed in Table 3. Because the instrument's response of the spectrometer used in this study is about 30 ps, the components of the observed solvation process in the whole solvation process are estimated by Fee and Maroncelli's method.[74] The magnitude of the observed solvation components

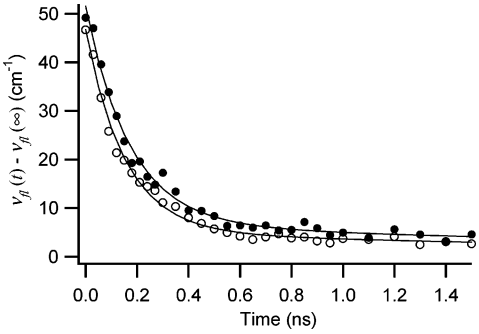

Figure 9. Time-dependent fluorescence maximum frequency shifts of C102 in 405 mM SDS micelle solutions (open circles for H_2O medium and filled circles for D_2O medium). Biexponential fit curves are also shown.

in this study are listed in Table 3. The missing solvation component should contain the faster solvation dynamics due to the contributions of the dynamics of free water molecules and the other faster dynamics of water in the interface between the Stern layer and bulk region. The notable points of the results of the solvation dynamics in SDS micelle solutions are (i) the time constants of the solvation dynamics are independent of the SDS concentration and (ii) the observed solvation component is increasing with the higher SDS concentration (Table 3).

Figure 9 shows the comparison between the solvation dynamics of C102 in SDS/H_2O and SDS/D_2O with [SDS] = 405 mM. The solvation dynamics in SDS/D_2O is slower than that in SDS/D_2O. The other SDS concentration sample ([SDS] = 16.2 mM) also shows the retardation of the solvation dynamics by deuterium isotopic substitution of the solvent medium. From the biexponential fit, the solvation time constants for SDS/D_2O are about 1.2 times larger than those for SDS/H_2O. The solvation dynamics parameters for the deuterated samples are also summarized in Table 3. Another fluorescence probe C153 also shows the similar deuterium isotope effect on the solvation dynamics in SDS micelle solutions.

4. Discussion

4.1. Static Properties. First of all, we discuss the features of the static solvation in SDS micelle solutions, because the steady-state absorption and fluorescence spectra contain important information of the microenvironment around the probe. The solvent reorganization energy λ_s can be estimated by the following equation.[75]

$$\lambda_s = (\Delta\nu - \Delta\nu_{ref})/2 \quad (4)$$

where $\Delta\nu$ and $\Delta\nu_{ref}$ are the fluorescence Stokes shifts in target polar solvents and in a reference nonpolar solvent (about 2200 cm^{-1} in cyclohexane). The $\Delta\nu$ for the coumarins in SDS micelle solutions is about 4250 cm^{-1}. The $\Delta\nu$ for C102 in methanol, ethylene glycol, and glycerol are 4450, 4320, and 4090 cm^{-1} and for C153 in methanol, ethylene glycol, and glycerol are 4800, 4630, and 4120 cm^{-1}. The solvent reorganization energy of the coumarins in SDS micelle solutions is between those in ethylene glycol and glycerol.

Because the micelle solutions are microheterogeneous, one might need to consider the microenvironment around the fluorescence probe molecule. The fluorescence spectra of the coumarins in SDS micelle solutions do not depend on the wavelength of the excitation light, as described above. The result indicates that each coumarins is in a similar microenvironment

of the solution in the fluorescence probing time scale. If we assume that the microenvironment of the coumarins is homogeneous, there are three possibilities of the coumarin's microenvironment in aqueous micelle solution: bulk water region, hydrophobic micelle core, and Stern layer. Because the steady-state absorption and fluorescence spectra of C102 in SDS micelle solution are different from those in pure H_2O, C102 should not be in the bulk water region. Further, the solubility of C153 in pure water is less. On the other hand, the coumarins could also not exist inside the SDS micelle hydrophobic core, because the steady-state fluorescence spectra show the microenvironment around the coumarins is very polar. The remaining possibility is the Stern layer. Because the micropolarity around the coumarins is rather high in comparison with the common organic solvents, the coumarins could be in the Stern layer. However, C102 is rather insoluble in the ionic environment (Figure 3). It can hardly be believed that the coumarins are freely in the Stern layer (without any interaction with the micelles). Therefore, one could think that the coumarins attach on the surface of SDS micelle in the fluorescence probing time scale. We also note that the thickness of the Stern layer and the axis size of coumarins used are competitive. Therefore, the bulklike water molecules should contribute to both the solvation and probe reorientation. We will further discuss the microenvironment of the coumarins in the later section.

As shown in Figure 2a, both the steady-state absorption and fluorescence spectra of C102 in SDS micelle solutions change dramatically in the critical micelle concentration. Above the critical micelle concentration, both the steady-state absorption and fluorescence spectra of C102 and C153 in SDS micelle solutions only slightly shift to the shorter wavelength. The fluorescence Stokes shifts of C102 and C153 become slightly smaller with the higher SDS concentration: 4230−4280 cm^{-1} for C102 and 4240−4310 cm^{-1} for C153 in SDS micelle solutions with [SDS] = 16.2−810 mM. The result indicates that the coumarins in SDS micelle solutions with the higher SDS concentration are more energetically stabilized than in the lower SDS concentration micelle solution. This is a trend opposite to the normal case, because the polarity of water is larger than that of the SDS micelle. We also observed the similar spectral feature in C153 in aqueous 1-propanol solutions: the larger $\Delta\nu$ with the larger 1-propanol mole fraction.[76] The origin of this feature in aqueous 1-propanol solutions should be due to the incomplete contribution of water for the solvent stabilization arising from the coumarin's strong hydrophobicity. However, we note that the SDS concentration dependence on the steady-state absorption and fluorescence spectra of C102 and C153 in SDS micelle solutions is very small.

The steady-state absorption and fluorescence spectra of the coumarins in SDS micelle H_2O and D_2O solutions are almost identical, as shown in Figure 4a. The steady-state absorption and fluorescence maxima of some solvatochromic fluorescence molecules in simple hydrogen-bonding liquids, such as water,[77,78] methanol,[78] and anilines,[79] also do not change by the deuterium isotopic substitutions of the hydrogen-bonding sources in hydrogen-bonding molecular liquids within experimental error. Although the present system is a complex micelle solution, the contribution of the medium deuterium substitutions is too small to affect on the static solvent reorganization energy of the coumarins, as well as simple hydrogen-bonding liquids.

4.2. Probe Reorientation in SDS Micelle Solutions. To understand the microenvironment around the fluorescence probe, the fluorescence anisotropy decays of coumarins in micelle solutions are investigated. The fluorescence anisotropy decay $r(t)$ of a fluorescence probe molecule in micelle solutions is often expressed by a biexponential function,

$$r(t) = r_0[(1-\beta)\exp(-t/\tau_{fast}) + \beta\exp(-t/\tau_{slow})] \quad (5)$$

where r_0 is the anisotropy at time zero. In the case of the coumarins, the value of the r_0 is close to 0.4.[80] The biexponential reorientation feature in micelle solutions is well analyzed by the wobbling-in-cone model,[81,82] including the lateral diffusive motion along the micelle surface.[83−90] Although it is possible to think that the biexponential anisotropy feature arises from the reorientational motion of the fluorescence probe and the micelle entire rotation, the time constant for the whole rotational motion of a micelle is much larger than the time constant obtained by the fluorescence anisotropy decay measurement (vide infra).

According to the wobbling-in-cone model including the lateral diffusion,[83] the anisotropy decay arises from the following three distinct motions: (i) the entire rotation of micelle, (ii) the translational diffusive motion of the dye along the spherical micelle surface, and (iii) the wobbling motion of the dye in a cone. The relationships of the time constants between the experimental observation and the model are

$$1/\tau_{slow} = 1/\tau_m + 1/\tau_t \quad (6)$$

and

$$1/\tau_{fast} = 1/\tau_w + 1/\tau_m + 1/\tau_t \quad (7)$$

where τ_m, τ_t, and τ_w are the time constants for the whole rotation of a micelle, the translational diffusive motion of the dye along the micelle surface, and the wobbling motion of the dye in a cone, respectively. The amplitude β is directly related to a generalized order parameter S: $\beta = S^2$. On the basis of the wobbling-in-cone model, S is given by

$$S = \cos\theta(1+\cos\theta)/2 \quad (8)$$

where θ is the semicone angle. Equation 5 can be rewritten by

$$r(t) = r_0\{S^2 + (1-S^2)\exp(-t/\tau_w)\}\exp\{-t/(\tau_t+\tau_m)\} \quad (9)$$

The reorientation time of the spherical micelle τ_m is calculated from the Stokes−Einstein−Debye equation.

$$\tau_m = \frac{4\pi r_m^{\,3}\eta}{3k_BT} \quad (10)$$

where r_m is the radius of the micelle, η is the medium viscosity, k_B is the Boltzmann constant, and T is the absolute temperature. Because the thickness of the Stern layer of the ionic micelle is about 0.6−0.9 nm,[7,91] the r_m in here is tentatively 2.0 nm (the average diameter of the micelle measured in this study is 5.6 nm). The translational diffusion time τ_t along the micelle surface converts to the diffusion coefficient D_t:

$$D_t = r_m^{\,2}/6\tau_t \quad (11)$$

The wobbling diffusion coefficient D_w is given by

$$D_w = \{\tau_w(1-S^2)\}^{-1}\{-x^2(1+x)^2[\ln\{(1+x)/2\} + (1-x)/2]/\{2(1-x)\} + (1-x)(6+8x-x^2-12x^3-7x^4)/24\} \quad (12)$$

where $x = \cos\theta$. The values of τ_{fast}, τ_{slow}, and β are used as

TABLE 4: Analytical Reorientation Parameters for C102 and C153 in SDS/H_2O and SDS/D_2O

dye	medium	τ_w (ps)	τ_t (ps)	τ_m (ns)	$\|S\|$	$10^9 D_t$ ($m^2\ s^{-1}$) (D_{tD}/D_{tH})	θ_0 (deg)	$10^{-9} Dw$ (s^{-1}) (D_{wD}/D_{wH})
C102	H_2O	78	529	7.3	0.648	1.26	42	1.68
	D_2O	85	589	9.0	0.707	1.13 (0.90)	38	1.31 (0.78)
C153	H_2O	80	597	7.3	0.671	1.12	40	1.49
	D_2O	83	652	9.0	0.693	1.02 (0.91)	39	1.41 (0.95)

the average τ_{r1}, τ_{r2}, and $a_{r2}/(a_{r1} + a_{r2})$ measured in the different concentration samples ([SDS] = 16.2 and 405 mM).

Table 4 summarizes the parameters analyzed by the above model for the reorientation of coumarins in SDS micelle solutions. The obtained parameters for coumarins in SDS micelle solutions are quite similar to those of tryptophan derivatives in SDS micelle solutions.[90] It is well suggested that the translational diffusion along the micelle surface of a probe is related to the self-diffusion of the surfactants. According to the NMR experiments, the values of the self-diffusion coefficients of surfactants are about 10^{-10} $m^2\ s^{-1}$.[92,93] Kelepouris and Blanchard reported that the D_t of the oppositely charged probe/micelle systems is similar to that of the self-diffusion coefficient of surfactant in micelle. Because the coumarins used in this study are interacted hydrophobically with the SDS micelles, the translational diffusions of the probes might be faster than the self-diffusion of the surfactant in micelle.

From the deuterium substitution study, it becomes clear that the entire micelle motion, the translational diffusive motion of the probe along the micelle surface, and the probe wobbling motion of C102 becomes slower by the deuterium isotopic substitutions of the medium solvent. The negligible deuterium isotope effect of C153 wobbling motion may be due to the strong hydrophobicity of C153. The result of the deuterium isotope effects on the translational and wobbling motions in SDS micelle solutions indicates that the frictions for the rotational and translational diffusions of the probes in the deuterated hydration layer around SDS micelle are larger than those in the undeuterated hydration layer around the micelle.

4.3. Solvation Dynamics in SDS Micelle Solutions. *4.3.1. SDS Concentration Dependence.* The micelle density and mean distance between micelles of the surfactant solution in the spherically assembly concentration region vary with the change of the surfactant concentration without the changes of the shape and diameter of micelle. To study the wide concentration range, we can understand the solvation dynamics of hydration water around micelles, which are isolated from the other micelles (dilute condition) and interact with the other micelles (concentrate condition). Because the dynamical model, which includes the effect of the interaction between micelles, is less, it will help for the detailed understanding of the hydration water dynamics.

The notable points of the experimental result of the SDS concentration dependence on the solvation dynamics in micelle solutions (Figure 8) are the following: (i) The observed solvation component is increasing with the higher SDS concentration of the micelle solutions [(C102) 0.23 for [SDS] = 16.2 mM and 0.29 for [SDS] = 810 mM; (C153) 0.18 for [SDS] = 16.2 mM and 0.26 for [SDS] = 810 mM]. (ii) The time constants for the solvation dynamics of the coumarins in SDS micelle solutions are independent of the SDS concentration within experimental error.

The shape and aggregation number of the micelles in the spherical micelle forming the concentration region of the solutions (8.1×10^{-3} to ~1.4 M in the case of SDS)[71] are not much varied by the change of the surfactant concentration. However, the number density of the micelles in solution varies by the change of the surfactant concentration. Namely, the component of bulk water in the micelle solution decreases and the fraction of hydration water in the micelle solution increases with the higher SDS concentration and the larger number density of micelle. When the aggregation number of the SDS micelle (74)[94] and the critical micelle concentration of SDS in water (8.1 mM)[71] are taken into consideration,[10] the mean distances between SDS micelles in water with [SDS] = 16.2 mM and 810 mM are about 21.6 and 5.3 nm, respectively (the ratio between the hydration space and the bulklike water region is ~0.95 for [SDS] = 810 mM and ~0.004 for [SDS] = 16.2 mM). Because the coumarins are probing of the microenvironment in micelle solution (micelle surface), it is not directly correlated with the ratio between the volume ratio of the Stern layer and bulklike water region. However, the qualitative feature of the SDS concentration dependence on the observed solvation component should come from the distance between micelle hydration layers.

On the other hand, both the faster and slower solvation time constants are almost independent of the SDS concentration, as well as the reorientation time constants of the fluorescence probe. Because the mean distance between micelle and micelle (and hydration layer and hydration layer) depends on the SDS concentration of the solution, it may change the intermolecular interactions of hydration water molecules around micelles. If the interaction strength in hydration water varies with the change of the SDS concentration, the solvation time constants arising from the hydration water should change. Therefore, the present result indicates that the interaction strength of hydration water around micelles is rather insensitive to the SDS concentration (distance between micelles). This solvation dynamics result is well consistent with the result of the probe reorientation.

4.3.2. Comparison between H_2O and D_2O Environments around Micelles. Because micelles are hydrophobically formed in water, the deuterium substitution of the medium water gives a different feature. For example, the critical micelle concentration in D_2O is lower than that in H_2O.[95] This feature occurs due to the hydrophobic effect. Here, the deuterium isotope effect on the solvation dynamics is examined to see the contribution of hydrogen bonds to the reorganization process of the hydration layer around micelles.

As shown in Figure 9, the solvation dynamics in SDS micelle D_2O solutions is slower than that in SDS micelle H_2O solutions. Both the faster and slower solvation time constants for SDS micelle D_2O solutions are about 1.2 times larger than those for SDS micelle H_2O solutions, as shown in Table 3. It is reported that the diffusive solvation dynamics of coumarins in simple hydrogen-bonding liquids, such as water,[96,97] methanol,[98] and anilines,[79,99,100] becomes slightly slower by the deuterium isotopic substitutions of the hydrogen-bonding sources. The similar deuterium isotope effect in hydrogen-bonding liquids was also observed in the dielectric relaxation[101] and polarizability anisotropy relaxation.[102,103]

Hydrogen bond becomes more stabilized by deuterium isotopic substitution, because the zero-point energy for the deuterated hydrogen bond is lower than that for the ordinary hydrogen bond due to the heavier mass of deuterium than that of hydrogen.[104] The making and breaking processes of the hydrogen bond thus becomes slower by the exchange from hydrogen to deuterium. As a result, the solvation dynamics and the other relaxation process related to the motion of hydrogen bonds in hydrogen-bonding liquids show the retardation by the deuterium isotopic substitutions of hydrogen-bonding sources.

In other words, the stabilized hydrogen bond by deuterium isotopic substitution gives the larger friction for the mobility of molecules and molecular collective motions.

Although aqueous micelle solution systems are not a simple hydrogen-bonding molecular system, the similar deuterium isotope effect on the solvation dynamics is observed in aqueous SDS micelle solutions. The present result indicates that the origin of the deuterium isotope effect on the solvation dynamics in aqueous SDS micelle solutions could be similar to that in simple hydrogen-bonding liquids though the dynamical feature of the hydration layer around micelle is very much different from that of bulk water. Though the hydrogen bond in the hydration layer around the micelle core is more stabilized than that in bulk water, the stabilization effect of the hydrogen bond by deuterium substitution is due to the different zero-point energies. This effect should give the similar retardations of the hydrogen-bonding making and breaking process in hydration water with bulk water and the exchange process between bulk water molecules and hydration water molecules. The similar deuterium isotope effect on the solvation dynamics of the hydration water in reverse micelles[35] and around nanoparticles[97] were also reported.

As well as the concentration dependence result, the deuterium isotope effect result shows some similarity between the solvation dynamics and the probe orientation dynamics in SDS micelle solutions. These results imply that the diffusive motions (translational motion along micelle surface and wobbling rotation) of adsorbed molecule on micelle are influenced by the collective motion of the hydration water. The collective motions of the biological hydration water might also affect on the mobility of protein, ion, and other molecules in biological lipid membrane, just like micelle case.

5. Conclusion

The solvation dynamics and orientational dynamics of coumarins 102 and 153 in SDS micelle solutions have been investigated using the picosecond time-resolved emission spectroscopy. In this study, we have focused on the SDS concentration dependence and the solvent deuterium isotope effect on the solvation dynamics. The observed solvation dynamics in SDS micelle solutions is expressed by a biexponential function (about 130 ps and 2.5 ns). Both the faster and slower solvation time constants are independent of the SDS concentration, whereas the observed solvation component is increasing with the higher SDS concentration of the solution. The experimental results suggest that the observed solvation component is coming from the amount of the hydration water of micelles. However, the interaction between the hydration layer and hydration layer could not depend on the SDS concentration, because both the faster and slower solvation time constants are insensitive to the SDS concentration. From the solvent deuterium substitution experiments, we have found that both the faster and slower solvation time constants in SDS micelle D_2O solutions are about 1.2 times larger than those in SDS micelle H_2O solutions. The solvation dynamics in the hydration layer around the hydrophobic micelle core is influenced by hydrogen bonds, as well as simple hydrogen-bonding liquids. The surfactant concentration dependence and solvent isotope effect on the orientational dynamics of the coumarins have also been investigated. The result of the orientational dynamics of the coumarins in aqueous micelle solutions has been analyzed by the wobbling-in-cone model including the lateral diffusion. Both the surfactant concentration dependence and solvent isotope effect on the orientational dynamics show features similar to those on the solvation dynamics. These results imply that the hydration water dynamics in micelles affects on the diffusive motions of the adsorbed molecule on the micelle.

Acknowledgment. We thank to Prof. Kankan Bhattacharyya (Indian Association for the Cultivation of Science) for fruitful discussion. The work is partially supported by the Shiseido Fund for Science and Technology and the Mitsubishi Chemical Corporation Fund (H.Shirota). We also acknowledge the Ministry of Education, Culture, Sports, Science and Technology of Japan (Gant-in-Aid for Scientific Research on Priority Areas: 417).

References and Notes

(1) Frank, H. S. *Water*; Plenum: New York, 1972.
(2) Jeffrey, G. A.; Saenger, W. *Hydrogen Bonding in Biological Structures*, 1st ed.; Springer-Verlag: Berlin, 1991.
(3) Kuntz, I. D. J.; Kauzmann, W. *Adv. Protein Chem.* **1974**, *28*, 239.
(4) Rupley, J. A.; Careri, G. *Adv. Protein Chem.* **1991**, *41*, 37.
(5) Teeter, M. M. *Annu. Rev. Biophys. Biophys. Chem.* **1991**, *20*, 577.
(6) Pethig, R. *Annu. Rev. Phys. Chem.* **1992**, *43*, 177.
(7) Nandi, N.; Bhattacharyya, K.; Bagchi, B. *Chem. Rev.* **2000**, *100*, 2013.
(8) Pal, S. K.; Peon, J.; Bagchi, B.; Zewail, A. H. *J. Phys. Chem. B* **2002**, *106*, 12376.
(9) *Physics of Amphiphiles: Micelles, Vesicles and Microemulsions*; Degiorgio, V., Corti, M., Eds.; North-Holland Physics Publishing: Amsterdam, 1985.
(10) Israelachvili, J. N. *Intermolecular and Surface Forces*, 2nd ed.; Academic Press: London, 1992.
(11) Barbara, P. F.; Jarzeba, W. *Adv. Photochem.* **1990**, *15*, 1.
(12) Maroncelli, M. *J. Mol. Liq.* **1993**, *57*, 1.
(13) Bagchi, B.; Biswas, R. *Adv. Chem. Phys.* **1999**, *109*, 207.
(14) Jarzeba, W.; Walker, G. C.; Johnson, A. E.; Barbara, P. F. *Chem. Phys.* **1991**, *152*, 57.
(15) Jimenez, R.; Fleming, G. R.; Kumar, P. V.; Maroncelli, M. *Nature* **1994**, *369*, 471.
(16) Horng, M. L.; Gardecki, J. A.; Frankland, S. J. V.; Maroncelli, M. *J. Phys. Chem.* **1995**, *99*, 17311.
(17) Reynolds, L.; Gardecki, J. A.; Frankland, S. J. V.; Horng, M. L.; Maroncelli, M. *J. Phys. Chem.* **1996**, *100*, 10337.
(18) Richert, R. *J. Chem. Phys.* **2000**, *113*, 8404.
(19) Bhattacharyya, K.; Bagchi, B. *J. Phys. Chem. A* **2000**, *104*, 10603.
(20) Bhattacharyya, K. *J. Fluoresc.* **2001**, *11*, 167.
(21) Bhattacharyya, K. *Acc. Chem. Res.* **2003**, *36*, 95.
(22) Levinger, N. E. *Curr. Opin. Colloid Interface Sci.* **2000**, *5*, 118.
(23) Sarkar, N.; Datta, A.; Das, S.; Bhattacharyya, K. *J. Phys. Chem.* **1996**, *100*, 15483.
(24) Datta, A.; Mandal, D.; Pal, S. K.; Das, S.; Bhattacharyya, K. *J. Mol. Liq.* **1998**, *77*, 121.
(25) Mandal, D.; Sen, S.; Bhattacharyya, K.; Tahara, T. *Chem. Phys. Lett.* **2002**, *359*, 77.
(26) Hara, K.; Kuwabara, H.; Kajimoto, O. *J. Phys. Chem. A* **2001**, *105*, 7174.
(27) Balasubramanian, S.; Bagchi, B. *J. Phys. Chem. B* **2001**, *105*, 12529.
(28) Balasubramanian, S.; Bagchi, B. *J. Phys. Chem. B* **2002**, *106*, 3668.
(29) Pal, S.; Balasubramanian, S.; Bagchi, B. *J. Chem. Phys.* **2002**, *117*, 2852.
(30) Zhang, J.; Bright, F. V. *J. Phys. Chem.* **1991**, *95*, 7900.
(31) Zhang, J.; Bright, F. V. *J. Phys. Chem.* **1992**, *96*, 5633.
(32) Zhang, J.; Bright, F. V. *J. Phys. Chem.* **1992**, *96*, 9068.
(33) Lundgren, J. S.; Heitz, M. P.; Bright, F. V. *Anal. Chem.* **1995**, *67*, 3775.
(34) Sarkar, N.; Das, K.; Datta, A.; Das, S.; Bhattacharyya, K. *J. Phys. Chem.* **1996**, *100*, 10523.
(35) Das, S.; Datta, A.; Bhattacharyya, K. *J. Phys. Chem. A* **1997**, *101*, 3299.
(36) Mandal, D.; Datta, A.; Pal, S. K.; Bhattacharyya, K. *J. Phys. Chem. B* **1998**, *102*, 9070.
(37) Pal, S. K.; Mandal, D.; Sukul, D.; Bhattacharyya, K. *Chem. Phys. Lett.* **1999**, *312*, 178.
(38) Riter, R. E.; Undiks, E. P.; Kimmel, J. R.; Levinger, N. E. *J. Phys. Chem. B* **1998**, *102*, 7931.
(39) Riter, R. E.; Willard, D. M.; Levinger, N. E. *J. Phys. Chem. B* **1998**, *102*, 2705.
(40) Riter, R. E.; Undiks, E. P.; Levinger, N. E. *J. Am. Chem. Soc.* **1998**, *120*, 6062.
(41) Willard, D. M.; Riter, R. E.; Levinger, N. E. *J. Am. Chem. Soc.* **1998**, *120*, 4151.

(42) Pant, D.; Riter, R. E.; Levinger, N. E. *J. Chem. Phys.* **1998**, *109*, 9995.
(43) Willard, D. M.; Levinger, N. E. *J. Phys. Chem. B* **2000**, *104*, 11075.
(44) Pant, D.; Levinger, N. E. *Langmuir* **2000**, *16*, 10123.
(45) Raju, B. B.; Costa, S. M. B. *Phys. Chem. Chem. Phys.* **1999**, *1*, 5029.
(46) Hazra, P.; Sarkar, N. *Chem. Phys. Lett.* **2001**, *342*, 303.
(47) Hazra, P.; Chakrabarty, D.; Sarkar, N. *Chem. Phys. Lett.* **2002**, *358*, 523.
(48) Hazra, P.; Sarkar, N. *Phys. Chem. Chem. Phys.* **2002**, *4*, 1040.
(49) Faeder, J.; Ladanyi, B. M. *J. Phys. Chem. B* **2000**, *104*, 1033.
(50) Faeder, J.; Ladanyi, B. M. *J. Phys. Chem. B* **2001**, *105*, 11148.
(51) Shirota, H.; Horie, K. *J. Phys. Chem. B* **1999**, *103*, 1437.
(52) Shirota, H.; Segawa, H. *Langmuir* **2004**, *20*, 329.
(53) Datta, A.; Pal, S. K.; Mandal, D.; Bhattacharyya, K. *J. Phys. Chem. B* **1998**, *102*, 6114.
(54) Pal, S. K.; Sukul, D.; Mandal, D.; Bhattacharyya, K. *J. Phys. Chem. B* **2000**, *104*, 4529.
(55) Pal, S. K.; Sukul, D.; Mandal, D.; Sen, S.; Bhattacharyya, K. *Tetrahedron* **2000**, *56*, 6999.
(56) Bursing, H.; Ouw, D.; Kundu, S.; Vohringer, P. *Phys. Chem. Chem. Phys.* **2001**, *3*, 2378.
(57) Benderskii, A. V.; Eisenthal, K. B. *J. Phys. Chem. B* **2000**, *104*, 11723.
(58) Benderskii, A. V.; Eisenthal, K. B. *J. Phys. Chem. B* **2001**, *105*, 6698.
(59) Benderskii, A. V.; Eisenthal, K. B. *J. Phys. Chem. A* **2002**, *106*, 7482.
(60) Vieceli, J.; Benjamin, I. *J. Phys. Chem. B* **2003**, *107*, 4801.
(61) Sen, S.; Sukul, D.; Dutta, P.; Bhattacharyya, K. *J. Phys. Chem. B* **2002**, *106*, 3763.
(62) Sen, S.; Dutta, P.; Sukul, D.; Bhattacharyya, K. *J. Phys. Chem. A* **2002**, *106*, 6017.
(63) Dutta, P.; Sen, S.; Mukherjee, S.; Bhattacharyya, K. *Chem. Phys. Lett.* **2002**, *359*, 15.
(64) Frauchiger, L.; Shirota, H.; Uhrich, E. K.; Castner, E. W., Jr. *J. Phys. Chem. B* **2002**, *106*, 7463.
(65) Zhong, D.; Pal, S. K.; Zewail, A. H. *Chemphyschem* **2001**, *2*, 219.
(66) Pal, S. K.; Peon, J.; Zewail, A. H. *Proc. Natl. Acad. Sci. U.S.A.* **2002**, *99*, 1763.
(67) Bruce, C. D.; Senapati, S.; Berkowitz, M. L.; Perera, L.; Forbes, M. D. E. *J. Phys. Chem. B* **2002**, *106*, 10902.
(68) Jancso, G.; Rebelo, L. P. N.; van Hook, W. A. *Chem. Rev.* **1993**, *93*, 2645.
(69) Shirota, H.; Horie, K. *Macromol. Symp.* **2004**, *207*, 79.
(70) Shirota, H.; Segawa, H. *J. Phys. Chem. A* **2003**, *107*, 3719.
(71) Kekicheff, P.; Grabielle-Madelmont, C.; Ollivon, M. *J. Colloid Interface Sci.* **1989**, *131*, 112.
(72) Fleming, G. R. *Chemical Applications of Ultrafast Spectroscopy*; Oxford University Press: New York, 1986.
(73) Siano, D. B.; Metzler, D. E. *J. Chem. Phys.* **1969**, *51*, 1856.
(74) Fee, R. S.; Maroncelli, M. *Chem. Phys.* **1994**, *183*, 235.
(75) van der Zwan, G.; Hynes, J. T. *J. Phys. Chem.* **1985**, *89*, 4181.
(76) Shirota, H.; Castner, E. W., Jr. *J. Chem. Phys.* **2000**, *112*, 2367.
(77) Shirota, H.; Kuwabara, N.; Ohkawa, K.; Horie, K. *J. Phys. Chem. B* **1999**, *103*, 10400.
(78) Shirota, H.; Ohkawa, K.; Kuwabara, N.; Endo, N.; Horie, K. *Macromol. Chem. Phys.* **2000**, *201*, 2210.
(79) Pal, H.; Nagasawa, Y.; Tominaga, K.; Kumazaki, S.; Yoshihara, K. *J. Chem. Phys.* **1995**, *102*, 7758.
(80) Horng, M. L.; Gardecki, J. A.; Maroncelli, M. *J. Phys. Chem. A* **1997**, *101*, 1030.
(81) Kinoshita, K., Jr.; Kawato, S.; Ikegami, A. *Biophys. J.* **1977**, *20*, 289.
(82) Kinoshita, K., Jr.; Ikegami, A.; Kawato, S. *Biophys. J.* **1982**, *37*, 461.
(83) Quitevis, E. L.; Marcus, A. H.; Fayer, M. D. *J. Phys. Chem.* **1993**, *97*, 5762.
(84) Wittouck, N.; Negri, R. M.; Ameloot, M.; De Schryver, F. C. *J. Am. Chem. Soc.* **1994**, *116*, 10601.
(85) Maiti, N. C.; Mazumdar, S.; Periasamy, N. *J. Phys. Chem.* **1995**, *99*, 10708.
(86) Maiti, N. C.; Krishna, M. M. G.; Britto, P. J.; Periasamy, N. *J. Phys. Chem. B* **1997**, *101*, 11051.
(87) Krishna, M. M. G.; Das, R.; Periasamy, N.; Nityananda, R. *J. Chem. Phys.* **2000**, *112*, 8502.
(88) Sen, S.; Sukul, D.; Dutta, P.; Bhattacharyya, K. *J. Phys. Chem. A* **2001**, *105*, 7495.
(89) Dutt, G. B. *J. Phys. Chem. B* **2002**, *106*, 7398.
(90) Kelepouris, L.; Blanchard, G. J. *J. Phys. Chem. B* **2003**, *107*, 1079.
(91) Berr, S. S.; Coleman, M. J.; Jones, R. R. M.; Johnson, J. S., Jr. *J. Phys. Chem.* **1986**, *90*, 6492.
(92) Ahlnas, T.; Soderman, O.; Hjelm, C.; Lindman, B. *J. Phys. Chem.* **1983**, *87*, 822.
(93) Nery, H.; Soderman, O.; Canet, D.; Walderhaug, H.; Lindman, B. *J. Phys. Chem.* **1986**, *90*, 5802.
(94) Cabane, B.; Duplessix, R.; Zemb, T. *J. Phys.* **1985**, *46*, 2161.
(95) Krescheck, G. C.; Schneider, H.; Scheraga, H. A. *J. Phys. Chem.* **1965**, *69*, 3132.
(96) Barbara, P. F.; Walker, G. C.; Kang, T. J.; Jarzeba, W. *Proc. SPIE* **1990**, *1209*, 18.
(97) Pant, D.; Levinger, N. E. *J. Phys. Chem. B* **1999**, *103*, 7846.
(98) Shirota, H.; Pal, H.; Tominaga, K.; Yoshihara, K. *J. Phys. Chem.* **1996**, *100*, 14575.
(99) Shirota, H.; Pal, H.; Tominaga, K.; Yoshihara, K. *J. Phys. Chem. A* **1998**, *102*, 3089.
(100) Pal, H.; Shirota, H.; Tominaga, K.; Yoshihara, K. *J. Chem. Phys.* **1999**, *110*, 11454.
(101) Kaatze, U. *Chem. Phys. Lett.* **1993**, *203*, 1.
(102) Chang, Y. J.; Castner, E. W., Jr. *J. Phys. Chem.* **1994**, *98*, 9712.
(103) Shirota, H.; Yoshihara, K.; Smith, N. A.; Lin, S.; Meech, S. R. *Chem. Phys. Lett.* **1997**, *281*, 27.
(104) Nemethy, G.; Scheraga, H. A. *J. Chem. Phys.* **1964**, *41*, 680.